ELSEVIER

Applied Surface Science 144–145 (1999) 64–68

applied surface science

Resolution and transfer width of thermal energy atomic scattering from solid surfaces (TEAS)

G. Varga *

Technical University of Budapest, Physical Department, Budafoki s 8, 1111 Budapest, Hungary

Abstract

The resolution of TEAS has been investigated as a function of energy spread of atomic beam. The model calculations have been executed within the framework of time dependent Schrödinger equation. The energy spread of realistic atomic beam has been taken into account by a wave-packet. The wave-packet describes the atomic beam as an ensemble of independent particles by quantum mechanics. Taking ideally periodic surface the resolution of diffraction peaks increases when the energy spread is decreased. This fact underlines the higher efficiency of the supersonic atomic source than the effusive atomic source. Furthermore the transfer width of experimental equipment increases—when the atomic beam monochromaticity is also increased—according to the concept of the transfer width. The relation between the transfer width and the size of the period of the surface topography significantly determines the resolution of the diffraction pattern.

Keywords: TEAS; Resolution; Transfer width

1. Introduction

The thermal energy atomic scattering from solid surfaces (TEAS) is an efficient method to investigate the very top layer of the surfaces [1]. TEAS provides information on surface structure, phonon spectra and impurity. In addition to these physical properties TEAS can describe the quantum processes on the solid surface. Present paper focuses on the question of the resolution and the transfer width of TEAS. The interaction of neutral atoms and solid surface is strictly quantum mechanical [2]. Time dependent Schrödinger equation (TDSE) is applied to describe the TEAS. The atomic beam is modelled by a wave-packet and the solid surface is characterised by an appropriate interaction potential. Solving the prescribed TDSE the wave-packet at the detector region provides the intensity distribution as the square of the absolute value of the final state. Clear-cut diffraction peaks are visible when the atomic beam is monochromatic enough and the surface is periodic. The concept of the transfer width [3] means the size on the solid surface from that the experimental setup is able to ensure information. Transfer width depends on the energy spread of the atomic beam, the angular spread of the source and of the detector, as well as the spread of the surface impurity. When the transfer width is greater than the typical period length of the surface then clear-cut diffraction peaks can be seen. In this paper the resolution of TEAS is discussed in

* Telefax: +36-1-242-43-16; E-mail: vargag@phy.bme.hu

0169-4332/99/$ - see front matter
PII: S0169-4332(98)00766-1

the framework of a TDSE based physical model on the He–W(112) system.

2. The physical model

A time dependent realistic model that has been chosen characterises the neutral particle–solid surface scattering quantum mechanically. The main components are the following: the Gaussian wavepacket to describe the incoming particle beam and the interaction potential without restriction of the periodicity and of the time independence. Basically quantum mechanics is able to account for the physical processes of TEAS. In certain conditions—e.g., the probe particles are heavy atoms—semiclassical model approach is appropriate [2]. The time dependent Schrödinger equation has been applied that corresponds to an initial value problem. The incoming atomic beam is described by a plane wave in standard models. The plane wave is an interpretation of an absolutely monoenergetic atomic beam, which has no spread of velocity and of energy. Hard corrugated wall model and the closed couple models are the most popular within the frame of the plane wave atomic beam. However, as is known the supersonic atomic beams have narrow FWHM (Full Width Half Maximum) in the velocity space, because the velocity of the atomic beam may reach a few 10-fold of the local sound velocity. The relative velocity spread is defined by $\Delta v/\langle v\rangle$, where Δv is the velocity spread and $\langle v\rangle$ is the mean value of the velocity. The relative velocity spread of the supersonic beam is usually about a few percent. Wide FWHM leads to low resolution of the diffraction order. The plane wave corresponds to the correct mean value of the velocity, but an incorrect (zero) spread of the velocity distribution of the atomic beam. The Gaussian

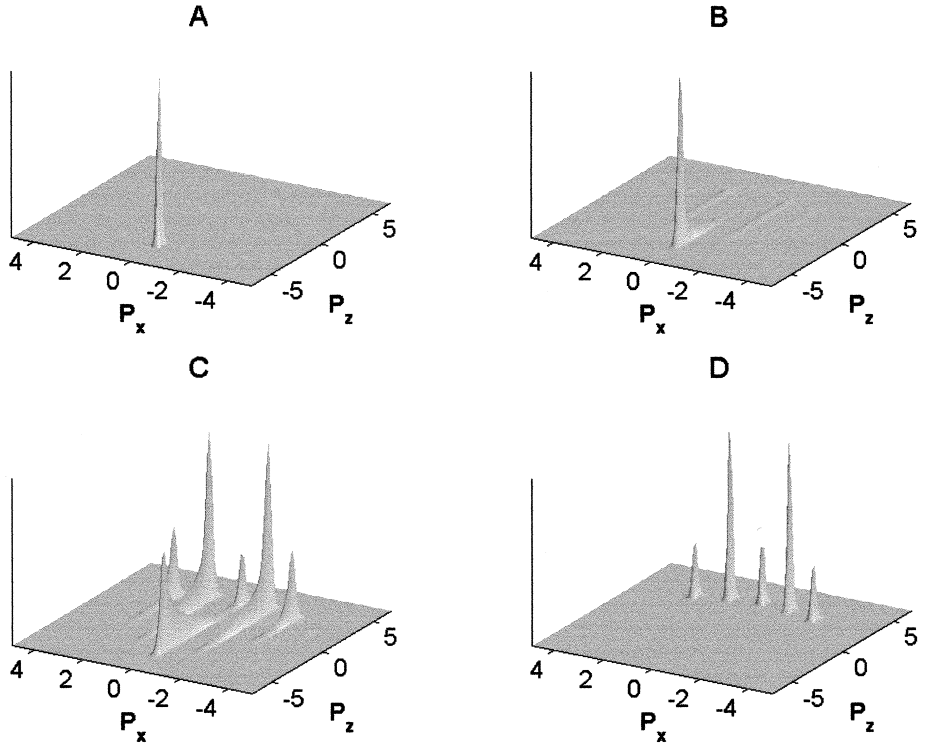

Fig. 1. Probability density functions (PDF) of He–W(112) scattering propagation in the momentum space. P_x and P_z are the momentum in direction x and z, respectively. Atomic units are used. (A) PDF is at the detector region (initial state). (B) and (C) PDF propagates in the interaction region. (D) PDF is at the detector region (final state).

wave packet provides proper mean velocity and velocity spread, but it does not mean correct velocity distribution. The Gaussian wave-packet can be considered as a description of an ensemble of neutral atoms with minimised uncertainty in real and momentum space. A more realistic wave-packet can be constructed from the velocity distribution of atomic beam that exits the skimmer [4] (it will be published later). What does the initial wave packet describe? It describes the collective behaviour of particles of the atomic beam. The particles of the atomic beam do not interact with each other, but they have a special distribution of the velocity and the energy. The Gaussian wave packet characterises the atomic beam as a special quantum ensemble of the independent particles. The wave packet gives exactly a 'collective' one particle system. 2D Gaussian wave-packet has been chosen as an initial wave function since W(112) has approximately one-dimensional surface corrugation:

$$\Psi(x, z, t=0) = C\exp\Big(-(x-x_0)^2/2\sigma_1^2 - (z-z_0)^2/2\sigma_3^2\Big)\exp(i\boldsymbol{kr}) \quad (1)$$

where Ψ is the wave function, (x, z) are Cartesian co-ordinates, t is the time, C is the normalisation constant, (x_0, z_0) is the average position at $t=0$, σ is the standard deviation of the space co-ordinate, 'i' is the complex unit, $\boldsymbol{k}$ is the wave number vector and $\boldsymbol{r}$ is the position vector. For describing the

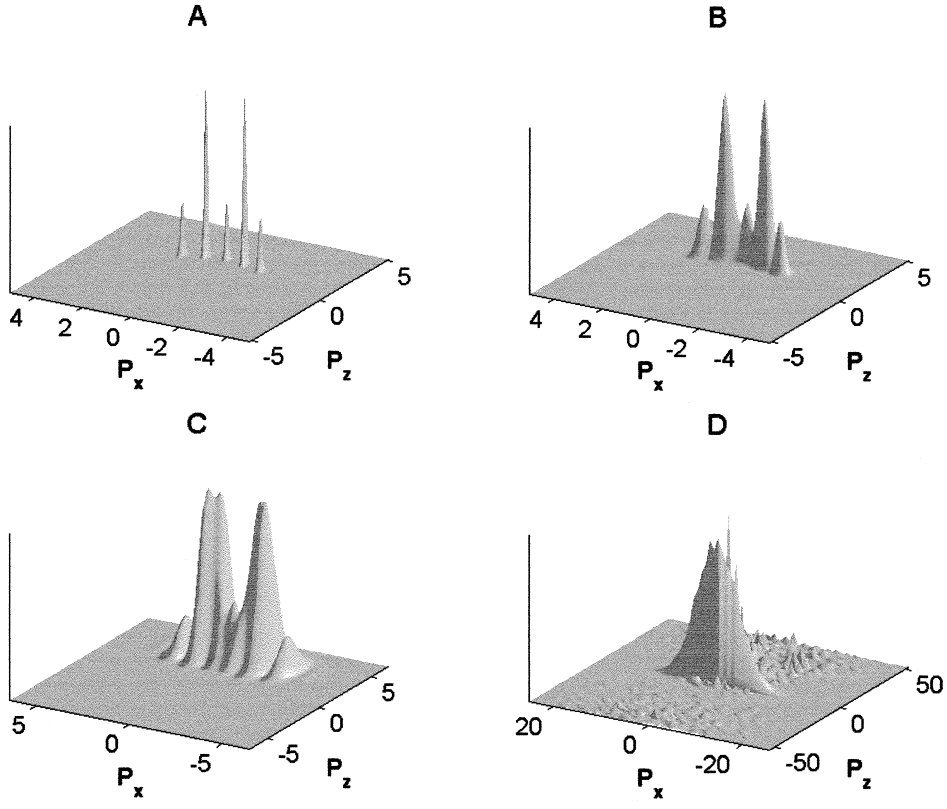

Fig. 2. Probability density functions (PDF) in the case of different relative velocity spreads (RVS) of initial wave function. P_x and P_z are the momentum in direction x and z, respectively. Atomic units are used. (A) RVS is 0 and 5% in direction x and z, respectively. (B) RVS is 5% in both directions. (C) RVS is 13% in both directions. (D) RVS is 80% in both directions.

interaction, the Lennard-Jones–Devonshire type potential has been chosen [5]:

$$V(x, z) = D\exp(-2\alpha z)\left\{1 - 2\beta\left[\cos\left(\frac{2\pi}{a}x\right)\right]\right\}, \quad (2)$$

where D is the energy constant, α is the repulsive constant, β is the corrugation constant and 'a' is the lattice constant.

3. Numerical method

Let us consider the time dependent Schrödinger equation: $i\hbar\frac{\partial\Psi(\mathbf{r},t)}{\partial t} = H\Psi(\mathbf{r}, t)$, where $\hbar$ is the Planck constant divided by 2π and H is the Hamiltonian. A propagation scheme and a Hamiltonian operation have to be applied. When splitting Hamilton operator for two parts, for kinetic energy operator A and potential energy operator B, we can write the exact formal solution: $\Psi(\mathbf{r}, t + \Delta t) = \exp[-i\Delta t(A + B)/\hbar]\Psi(\mathbf{r}, t)$, in the case of time independent potential. The solution of TDSE demands propagation scheme in every time step and requires a method that determines the effect of Hamilton operator for the wave function. We chose an efficient splitting operator method with third-order accurate formula in time [6–9] and the Fast Fourier transformation (FFT) has been applied to calculate $H\Psi$ in every time step [10].

4. Results

The standard deviation of the incoming wave-packet and the period of the surface are changed and the diffraction pattern is computed and visualised. The main data of the computations are the following

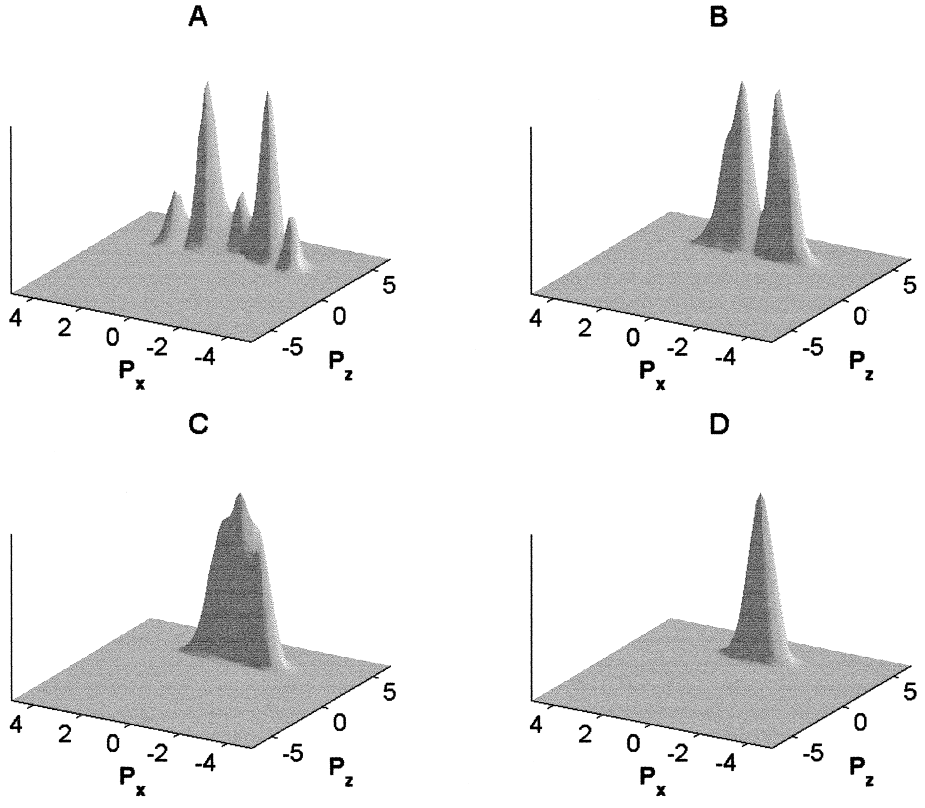

Fig. 3. Probability density functions (PDF) in the case of different lattice constants. P_x and P_z are the momentum in direction x and z, respectively. The relative velocity spread of initial wave function is 5% in both directions. (A) Lattice constant is 5.18 (a.u.). (B) Lattice constants is 10 (a.u.). (C) Lattice constant is 13 (a.u.). (D) Lattice constant is 20 (a.u.).

(in atomic units (a.u.)): in Eq. (1): $k_x = 0$, $k_z = -4$, in Eq. (2): $D = 0.00012$, $\alpha = 0.582$, $\beta = 0.2$. The base of the model calculations is the result in Appendix A: the energy spread is the inverse ratio to the co-ordinate spread. Fig. 1 shows the different stages of the probability density functions (PDF) of the scattering in the momentum space when (in a.u.): $\sigma_1 = \infty$, $\sigma_3 = \sqrt{5}$ and $a = 5.18$. Fig. 1A and D correspond to the atomic source region and the detector region, respectively. An almost monoenergetic beam can be seen in Fig. 1A. One can see the clear-cut diffraction peaks in Fig. 1D. Fig. 1B and C show the propagation of PDF during the scattering. If the transfer width is greater than the typical size of the period of a surface; diffraction peaks appear. Two types of model computations are executed. First the period of the surface is constant and the energy spread of the beam is changed. This case is shown in Fig. 2. In the order of A, B, C and D the monochromaticity of the atomic beam is decreased. The relative velocity spread of initial wave function has been determined by the help of Heisenberg inequality. In Fig. 2A and B there are narrow diffraction peaks. These correspond to the supersonic atomic source. There are greater FWHMs of diffraction peaks in Fig. 2C. Fig. 2D does not show a structured intensity distribution. The transfer width is less than the period of the surface. In second case (see Fig. 3) the period of the surface is changed and the energy spread of the beam is constant. In Fig. 3A, the peaks are well defined. The peaks of the intensity distribution disappear when the lattice constant of the surface is increased. The diffraction peaks overlap each other in Fig. 3B and C. The resolution is abruptly decreased as the lattice constant is increased. In Fig. 3D there is trace of only the specular peak. The result is a narrower peak than in Fig. 3C.

The above results support the idea that the transfer width have to be significantly greater than the surface period. Otherwise, the resolution of the experiment is not fine enough to determine the exact surface structure.

Appendix A

Let us investigate the relationship between the spread of co-ordinate x and kinetic energy. Let the normalised wave function be equal to: $\Psi(x) = [2\pi(\Delta x)^2]^{-\frac{1}{4}} \exp\left[-\frac{(x-\langle x\rangle)^2}{4(\Delta x)^2} + \frac{i}{\hbar}\langle p\rangle x\right]$, where x is the space co-ordinate, p is the momentum co-ordinate, $\langle\rangle$ and Δ denotes average and spread, respectively. The wave function is in the asymptotic region (at the atomic beam source)—outside of the interaction region—where the Hamiltonian contains only kinetic energy operator. Based on operator form of the Heisenberg inequality:

$$\Delta x \Delta E \geq \frac{1}{2}\left|\int_{-\infty}^{\infty} \Psi^* [x, H] \Psi \, \mathrm{d}x\right|$$

$$= \frac{\hbar^2}{2m}\left|\int_{-\infty}^{\infty} \Psi^* \frac{\partial \Psi}{\partial x} \mathrm{d}x\right| = \frac{|\langle p\rangle|\hbar}{2m},$$

where m is the particle mass, and E is the energy. One can see the energy spread is inversely proportional to the co-ordinate x spread.

References

[1] G. Comsa, Surf. Sci. 299/300 (1994) 77.
[2] B. Gumhalter, K. Burke, D.C. Langreth, On the Validity of the Trajectory Approximation in Quasi-Adiabatic Atom-Surface Scattering, 3S Symposium on surface science, Obertraun, Austria, 1991.
[3] G. Comsa, Surf. Sci. 81 (1979) 57.
[4] B.B. Hamel, D.R. Willis, Phys. Fluids 9 (1966) 829.
[5] A.T. Yinnon, R. Kosloff, Chem. Phys. Lett. 102 (1983) 216.
[6] A.D. Bandrauk, H. Shen, Chem. Phys. Lett. 176 (1991) 428.
[7] G. Varga, Seventh Joint Vacuum Conference, Debrecen, Hungary (JVC7), Extended Abstracts, 1997, p. 227.
[8] M. Suzuki, J. Math. Phys. 32 (1991) 400.
[9] A. Rouhi, J. Wright, Comput. Phys. 9 (1995) 554.
[10] H.J. Nussbaumer, Fast Fourier Transformation and Convolution Algorithms, Springer-Verlag, 1981.